ELSEVIER

PII: S0032-3861(97)00158-4

Polymer Vol. 38 No. 24, pp. 6001–6007, 1997

0032-3861/97/$17.00+0.00

Biodegradable polymer blends of poly(3-hydroxybutyrate) and hydroxyethyl cellulose acetate

Lianlai Zhang*† and Xianmo Deng
Chengdu Institute of Organic Chemistry, Academia Sinica, PO Box 415, Chengdu 610041, People's Republic of China

and Shujie Zhao
Chengdu Institute of Biology, Academia Sinica, Chengdu 610041, People's Republic of China

and Zhitang Huang
†Institute of Chemistry, Academia Sinica, Beijing 100080, People's Republic of China
(Revised 5 February 1997)

The melting and crystallization behaviour and phase morphology of poly(3-hydroxybutyrate) (PHB) and hydroxyethyl cellulose acetate (HECA) blends prepared by casting films have been studied by differential scanning calorimetry (d.s.c.), Fourier transform infra-red (*FT*i.r.), scanning electron microscopy and polarizing optical microscopy. The melting temperatures of PHB in the blends were independent of the blend composition with PHB contents above 20%. The melting enthalpy of the blends decreased with increase in the HECA component and was close to the additive value of the enthalpy of the two components. The glass transition temperatures of PHB in the blend were constant at about 8°C. No specific interaction between the two components was found by *FT*i.r. The crystallization of PHB in the blend was affected by the HECA component, especially in the PHB/HECA (20/80) blend. During the d.s.c. cooling run at a lower cooling rate, two separate transitions were found for PHB/HECA (80/20), (60/40) and (40/60) blends, which corresponded to the crystallization of PHB and the phase transition of HECA from an isotropic phase to a mesophase in the blends, respectively. The phase transformation of HECA from an isotropic phase to a mesophase was almost independent of the PHB component.

(Keywords: poly(3-hydroxybutyrate); hydroxyethyl cellulose acetate; blend)

INTRODUCTION

Poly(3-hydroxybutyrate) (PHB) is a naturally occurring crystalline polyester with optical activity. Now, it is produced by bacterial fermentation and is commercially available[1,2]. PHB can be degraded to water and carbon dioxide under environmental conditions by a variety of bacteria, and has much potential for applications of environmentally degradable plastics[3]. Its general characteristics are comparable to those of isotactic polypropylene[4]. Both polymers are crystalline with similar melting points, degrees of crystallinity and glass transition temperatures[5]. However, it is reported to be relatively hard and brittle, and its melting behaviour is unstable with a narrow thermal processing window[5]. Two main approaches have been extensively studied to obtain useful new derivatives based on PHB. One is the biosynthesis of copolyesters containing 3-hydroxyalkanoate units other than the 3-hydroxybutyrate unit, using one of several different kinds of bacteria[6]. The PHB copolymers with high comonomer content are thermally more stable and exhibit progressively large processing windows. Moreover, the mechanical properties of PHB can also be improved by this approach. However, both PHB homopolymer and copolymers are more expensive than conventional plastics[7]. Blending PHB with other polymers may offer opportunities to modify the physical properties, improve the processability and lower cost.

So far, many blends containing PHB have been studied[8]; however, among these, only blends with poly(ethylene oxide)[9–13], poly(vinyl alcohol) (PVA)[14,15], poly(L-lactide)[16], poly(D,L-lactide) (PDLLA)[17], poly(ε-caprolactone) (PCL)[18–21], poly(β-butyrolactone)[22–24] and poly(3-hydroxybutyrate-co-3-hydroxyvalerate)[25–28] are totally biodegradable. Polysaccharides, such as cellulose and starch derivatives, are natural polymers, and also biodegradable. Scandola and co-workers[29–31] have reported the miscibility, thermal and viscoelastic properties and biodegradation of PHB/cellulose acetate butyrate and cellulose acetate propionate blends.

Over years, we have focused on the biodegradable polymer blends containing PHB and PDLLA, PCL, poly(ester ether)s and cellulose derivatives[17,20]. Recently, a new cellulose derivative, hydroxyethyl cellulose acetate

*To whom correspondence should be addressed. Present address: Department of Chemistry, National University of Singapore, Singapore 119260

(HECA) was prepared, and its thermotropic behaviour has been studied[32]. We expect that the PHB/HECA blend can be found some applications as a new biodegradable material. Firstly, the thermal behaviour and phase morphology of the blends, which may affect the mechanical properties and biodegradation behaviour, as we have found in other biodegradable polymer blends, should be studied. Hence, this paper focuses on the melting and crystallization behaviour and phase morphology of biodegradable polymer blends of PHB and HECA.

EXPERIMENTAL

Materials

PHB, obtained from the Chengdu Institute of Biology, Academia Sinica, was prepared via bacterial fermentation using methanol as carbon source by methylotrophic strain 8502-3. The strain was selected from 100 strains of methanol-utilizing bacteria, named as *Hyphomicrobium zavarzinii* subsp. *chengduense* subsp. *nov.*[33]. The PHB production was performed with both feed batch and continuous fermentation. The high molecular weight PHB, ranging from 0.9×10^6 to 1.3×10^6 as determined by gel permeation chromatography (g.p.c.), was obtained from methanol. The PHB content of cells ranging from 40 to 59% was found with the highest productivity of $0.64\,g\,l^{-1}\,h^{-1}$. The crude product was dissolved in chloroform, filtered and then precipitated into methanol. The precipitate was filtered and dried under vacuum. The weight average molecular weight was 2.3×10^5 as determined by intrinsic viscosity measurement

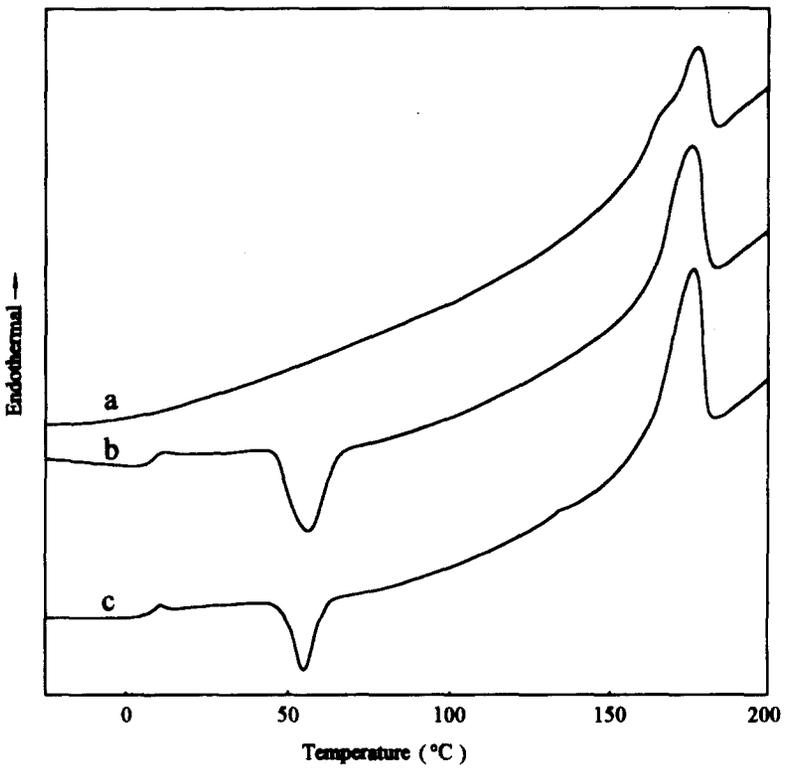

Figure 1 D.s.c. thermograms for PHB/HECA (80/20) blend (H8) during heating runs at a rate of $20°C\,min^{-1}$: (a) run I; (b) run III; (c) run V

Table 1 Melting temperature (T_m,°C), melting enthalpy (ΔH_f, $J\,g^{-1}$) and glass transition temperature (T_g,°C) of PHB, HECA and PHB/HECA blends in d.s.c. heating runs

Sample code	Composition (PHB/HECA)	Run I[a]		Run III[b]			Run V[c]		
		T_m	ΔH_f	T_g	T_m	ΔH_f	T_g	T_m	ΔH_f
H10	100/0	175.3	76.8	9.64	173.0	69.2	—	169.8	73.1
H8	80/20	175.9	67.1	9.12	174.8	62.7	8.50	173.4	62.4
H6	60/40	175.0	46.8	8.45	174.0	46.2	9.92	172.6	46.0
H4	40/60	175.1	35.1	7.87	174.3	30.8	8.06	172.4	32.2
H2	20/80	167.3	15.4	—	167.1	3.28	—	165.6	3.04
H0	0/100	166.3[d]	3.03[e]	—	164.9[d]	5.04[e]	—	161.6[d]	3.64[e]

[a] Obtained from original samples
[b] Obtained from samples after d.s.c. cooling run at a rate of $100°C\,min^{-1}$
[c] Obtained from samples after d.s.c. cooling run at a rate of $20°C\,min^{-1}$
[d] The temperature of the phase transformation from a mesophase to an isotropic phase, T_{mi}
[e] The enthalpy of the phase transformation from a mesophase to an isotropic phase, ΔH_{mi}
— No results available

using the relationship $[\eta] = 1.18 \times 10^{-4} \bar{M}_w^{0.78}$ in chloroform at 30°C[34]. HECA was prepared from hydroxyethyl cellulose according to the literature method[32]. The oxygen content of HECA was 42.75% as measured by elementary analysis using a Carlo Erba 1106 element analyser. The molecular weight of HECA was determined by g.p.c. using a Waters Associates ALC/GPC 244 apparatus at room temperature, with tetrahydrofuran as solvent, calibrated by polystyrene standards. The $\bar{M}_n$ and $\bar{M}_w$ were 4.7×10^4 and 3.1×10^5, respectively.

Preparation of blends

Thin films of PHB/HECA blends with weight ratios of 100/0, 80/20, 60/40, 40/60, 20/80 and 0/100 were prepared by casting from a 3% (w/v) solution of the two components in chloroform, allowing the solvent to evaporate at room temperature overnight, then keeping at 40°C under vacuum for 48 h.

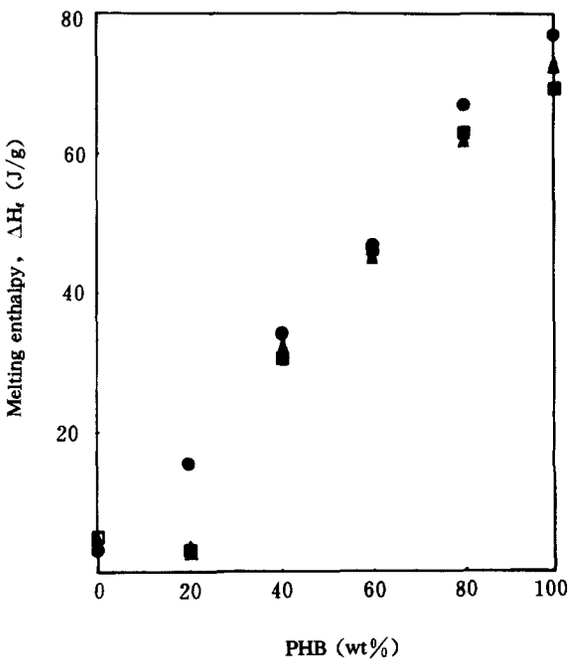

Figure 2 Melting enthalpy of PHB/HECA blends (ΔH_f) as a function of the blend composition: (●) run I; (■) run III; (▲) run V

Differential scanning calorimetry (d.s.c.)

The d.s.c. analysis was performed to study the thermal behaviour of the blends, on a Perkin Elmer DSC 7 apparatus equipped with a PE 3700 data station. The apparatus was calibrated with an indium standard, and a nitrogen atmosphere was used throughout. Samples as casting films were first heated from −60 to 200°C at a heating rate of 20°C min^{-1} (run I). The melting temperatures (T_ms) and apparent melting enthalpy (ΔH_f) were determined from d.s.c. endothermal peaks. After 1 min, samples were then cooled to −60°C at a cooling rate of 100°C min^{-1} (run II) to obtain specimens with lower crystallinity or totally amorphous specimens. Run III was a heating run at a rate of 20°C min^{-1} to 200°C; after 1 min, this was followed by run IV, cooling the samples to −60°C again at a rate of 20°C min^{-1}. The temperatures of crystallization (T_cs) and enthalpy of crystallization (ΔH_c) were determined from d.s.c. exothermal peaks in run IV. Finally, the samples were reheated to 200°C (run V). The T_m, ΔH_f, temperatures of cold crystallization (T_{cc}s) and enthalpy of cold crystallization (ΔH_{cc}) were obtained from runs III and V. The temperatures and enthalpy of the phase transformations of HECA from a mesophase to an isotropic phase (T_{mi}, ΔH_{mi}) and from an isotropic phase to a mesophase (T_{im}, ΔH_{im}) were also obtained from runs I–V for some samples.

The T_m, T_c, T_{cc}, T_{mi} and T_{im} were taken as the peak values of the respective endothermal or exothermal processes in the d.s.c. curves. In the presence of multiple endothermal peaks, the maximum peak temperature was taken as T_m. The T_g was taken as the midpoint of the specific heat increment.

Fourier transform infrared spectroscopy (FTi.r.)

The *FT*i.r. spectra were obtained with a Nicolet MX-1 i.r. spectrometer at room temperature. A total of 27 scans were taken with a resolution of 2 cm^{-1} in all cases.

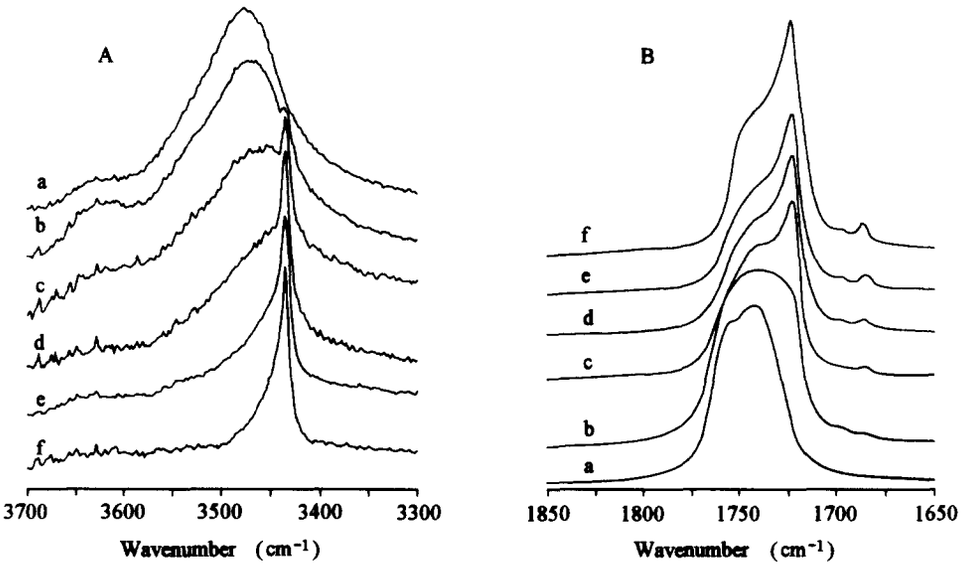

Figure 3 *FT*i.r. spectra of PHB, HECA and PHB/HECA blends at both hydroxyl (A) and carbonyl (B) regions: (a) HECA; (b) H2; (c) H4; (d) H6; (e) H8; (f) PHB

Samples were prepared by casting 3% (w/v) solutions directly onto KBr pellets, allowing the solvent to evaporate at room temperature, and then vacuum drying at 40°C overnight.

Polarizing optical microscopy

A Leitz Wetzlar Ortholux II POL-BK microscope equipped with a hot stage was used to observe the mesophase texture of HECA, and the crystallization and growth of spherulite of PHB in the blends. Samples cut from the casting films were first heated to 220°C, then cooled rapidly to the desired temperature and allowed to crystallize isothermally under crossed polars.

Scanning electron microscopy (SEM)

SEM was performed with an Amray 1000B equipment operated at 15 kV to examine the phase morphology. The blend films after methanol etching were used for surface observation. Before observation, all samples were coated with a thin layer of gold by means of a polaron sputtering apparatus.

RESULTS AND DISCUSSION

Melting behaviour and blend morphology

The d.s.c. studies were conducted to reveal the melting behaviour of PHB/HECA blends; typical d.s.c. curves during heating runs are shown in *Figure 1*. The d.s.c. results are recorded in *Table 1*. From the data of run I in *Table 1*, it is found that the melting temperatures (T_ms) of PHB in the blends are independent of the blend composition except for the PHB/HECA (20/80) blend (H2). The melting process of PHB in the H2 sample is significantly affected by the presence of the phase transformation of HECA from a mesophase to an isotropic phase, at about the same temperature region; thus the T_m of PHB shows a marked depression. The melting enthalpy of the blends (ΔH_f) decreases with increase in the HECA component. As displayed in *Figure 2*, it is close to the additive value of the enthalpy of phase transitions of the two components, calculated by the following relation:

$$\Delta H_f = \Delta H_f^{PHB} \times W^{PHB} + \Delta H_{mi}^{HECA} \times W^{HECA} \quad (1)$$

where ΔH_f and ΔH_f^{PHB} are the melting enthalpies of the blend and pure PHB, respectively, ΔH_{mi}^{HECA} is the enthalpy of the phase transformation of HECA from a mesophase to an isotropic phase and W^{PHB} and W^{HECA} are the weight fractions of PHB and HECA in the blends, respectively. Similar results are obtained in runs III and V except for the H2 sample (see *Figure 2*).

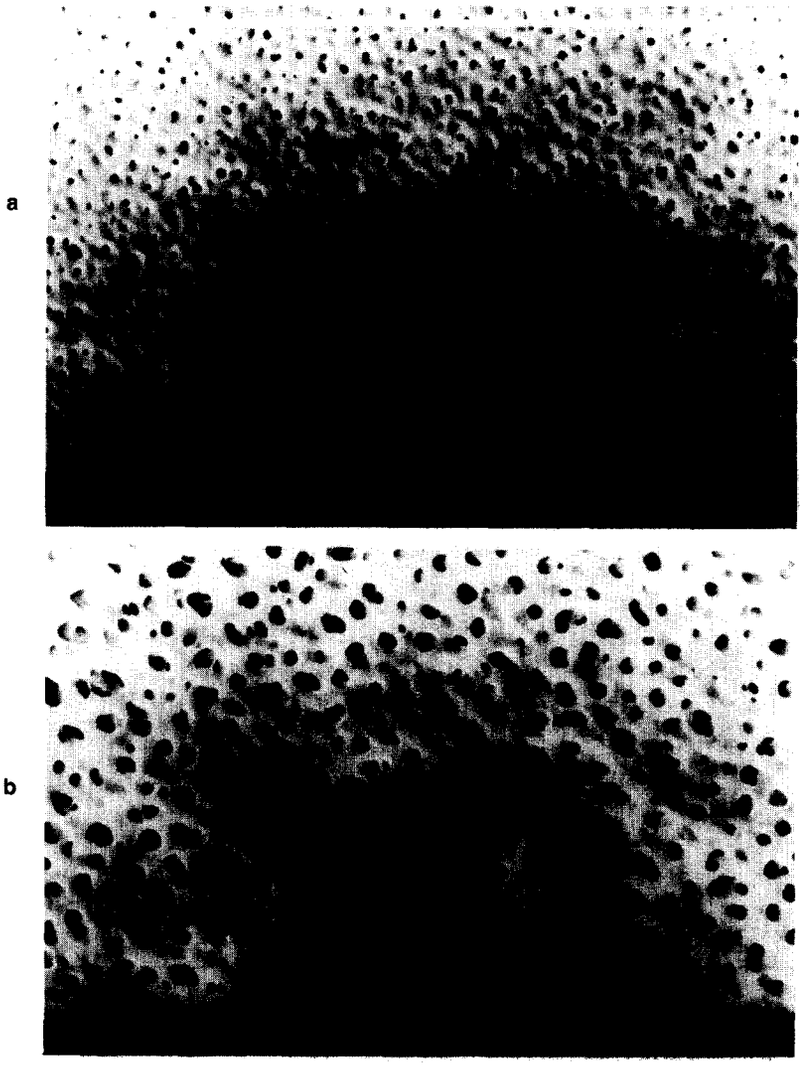

Figure 4 Scanning electron micrographs of the blend films etched with methanol: (a) H8; (b) H6

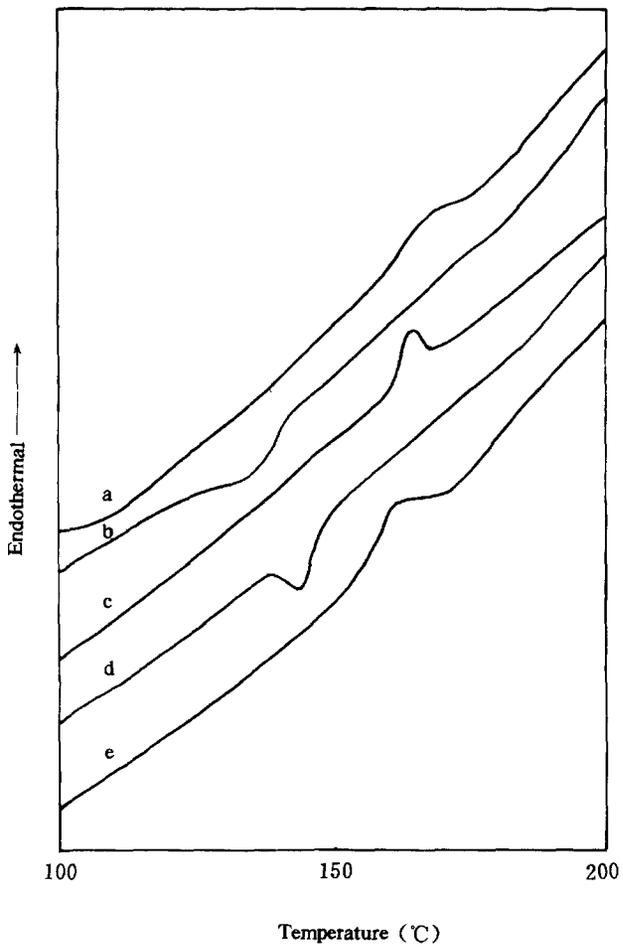

Figure 5 D.s.c. traces of HECA sample on heating and on cooling: (a) run I; (b) run II; (c) run III; (d) run IV; (e) run V

The glass transition temperatures (T_gs) of PHB in the blends can be determined by heating the samples after the d.s.c. cooling run; the results are shown in *Table 1*. In both runs III and V, the T_gs are constant at about 8°C. Because no clear glass transition of HECA is found, it is difficult to draw conclusions from these data. *FT*i.r. is further used to examine the possible interactions between hydroxyl groups of HECA and carbonyl groups of PHB. As shown in *Figure 3*, the absorption of hydroxyls in HECA is strong and broad at 3477 cm^{-1}, while the absorption of hydroxyl end groups of PHB is weak and sharper at 3436 cm^{-1}. In PHB/HECA blends, the O–H stretching bands of HECA remain at almost the same region of pure HECA. Furthermore, the absorption of carbonyl groups of PHB is independent of HECA content at 1724 cm^{-1}, and the C=O stretching of carbonyl groups of HECA is also constant at 1741 cm^{-1}. The results show that the hydrogen bonding in HECA is so strong that the interaction between PHB and HECA is very weak.

The scanning electron micrographs of H8 and H6 blends, taken after methanol etching to remove the HECA phase, are shown in *Figure 4*. The sizes of the etching phase are about 0.8 μm for H8, and 1 μm for H6. It is expected that the difference in morphology of the blends with different blend ratios would show an effect on the degradation behaviour of the blends.

Crystallization behaviour

HECA has been found to be an anisotropic liquid between 130 and 185°C on heating, and 150 and 105°C on cooling[32]. In this study, the temperature regions of the transformations are much narrower, as shown in *Figure 5*.

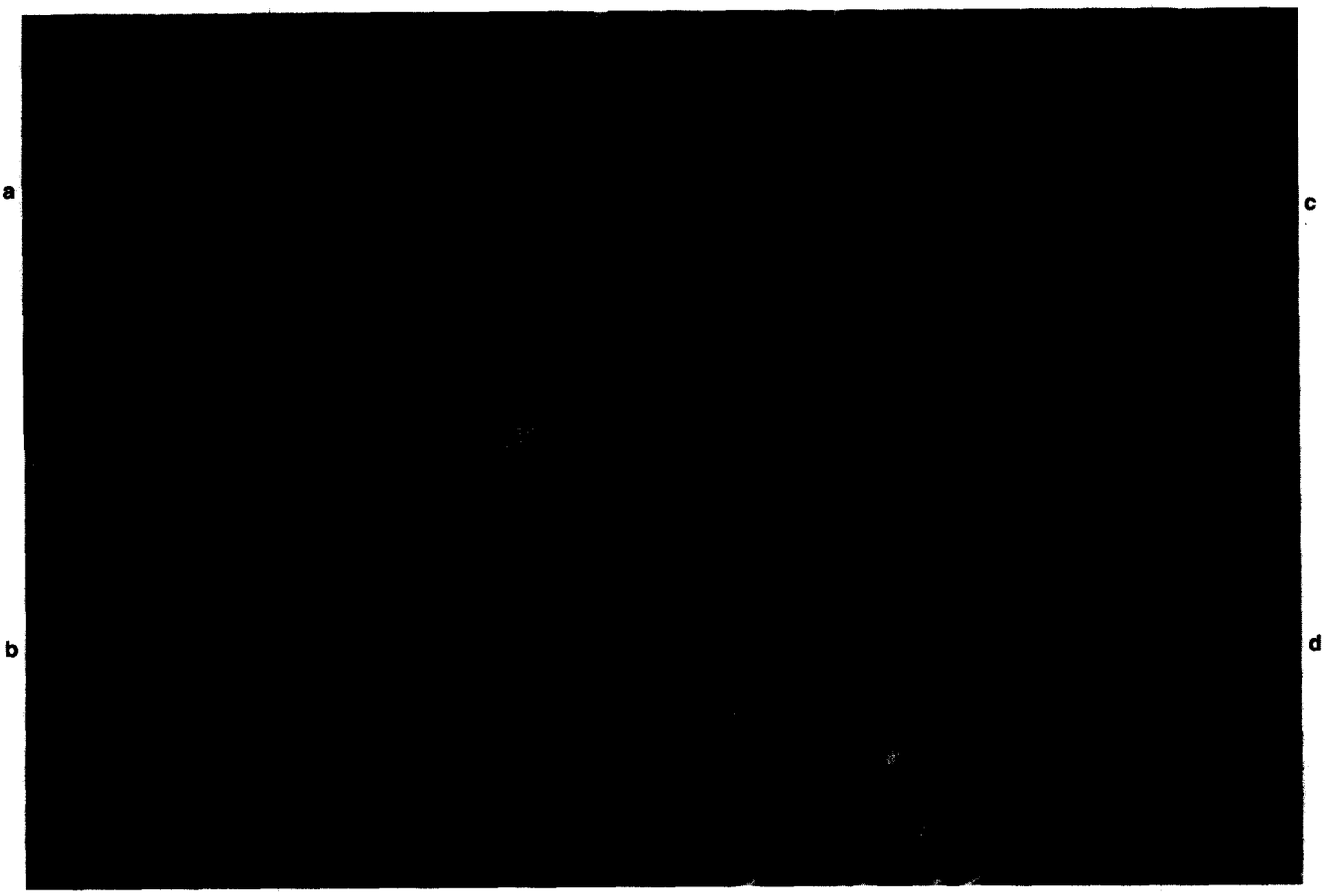

Figure 6 Polarizing optical micrographs of PHB, HECA and PHB/HECA blends under crossed polars (same magnification, magnification factor 128): (a) PHB; (b) H8; (c) H4; (d) HECA

An endothermal peak appears at 155–175°C on heating (*Figure 5a*), and an exothermal peak at 155–115°C on cooling (*Figure 5b*), corresponding to the transformations from a mesophase to an isotropic phase and an isotropic phase to a mesophase, respectively. The isothermal transformation of HECA from isotropic phase to mesophase was also observed under crossed polars at 80°C. The mesophase texture of HECA is shown in *Figure 6d*.

The isothermal crystallization of PHB, H8 and H4 blends was also observed using polarizing optical microscopy. From *Figure 6a*, it is found that well-defined spherulite is present at 80°C for plain PHB. In the H8 blend, PHB can also crystallize according to a spherulitic morphology, and large spherulites are observed in this case (*Figure 6b*). In the H4 blend, which contains 60% HECA, although the crystallization of PHB can be observed, no large spherulite is found with HECA as a second phase filling in the PHB lamellae (*Figure 6c*).

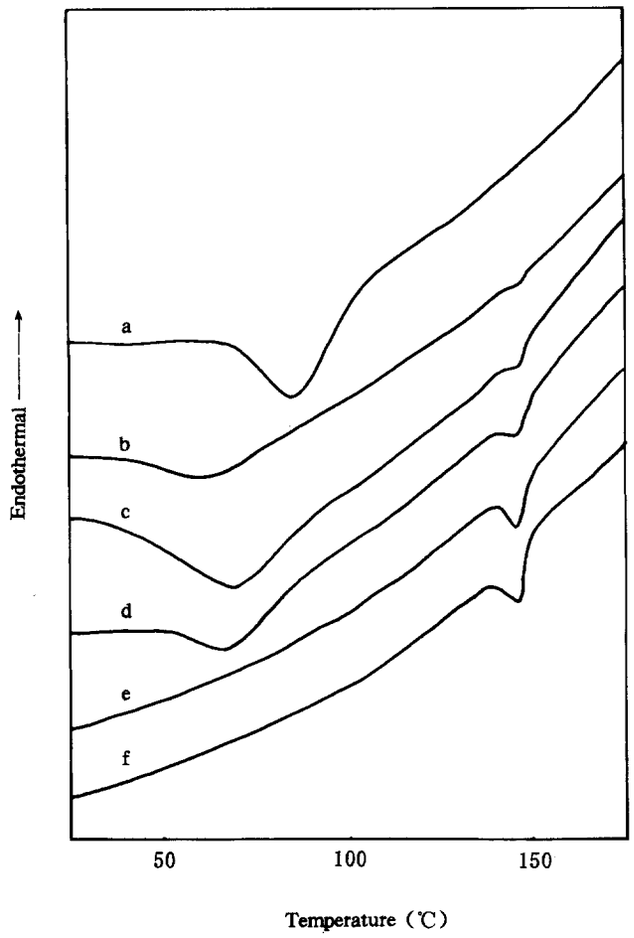

Figure 7 D.s.c. curves for PHB, HECA and PHB/HECA blends during cooling run at a rate of 20°C min^{-1}: (a) PHB; (b) H8; (c) H6; (d) H4; (e) H2; (f) HECA

The non-isothermal crystallization of PHB from the melt was studied by d.s.c. at two different cooling rates. The phase transformation from an isotropic phase to a mesophase of HECA is easier than the crystallization process, and can be found at both lower and higher cooling rates for pure HECA (see *Figures 5b* and *d*) and H2 blend. Unlike the phase transformation of HECA, the crystallization of PHB is strongly dependent on the cooling rates as well as the blend composition. Under a lower cooling rate of 20°C min^{-1}, pure PHB, H8, H6 and H4 samples can crystallize (see *Figure 7*); the results are summarized in *Table 2*. Because the higher cooling rate is unable to allow the specimen to crystallize at close to the equilibrium tranformation temperature, at a cooling rate of 100°C min^{-1}, pure PHB crystallizes incompletely with a much lower enthalpy of crystallization. No crystallization of PHB in the blends occurs at a higher cooling rate, indicating the effect of HECA on the crystallization of PHB. Two exothermal peaks appear in the d.s.c. traces of H8, H6 and H4 blends during the d.s.c. cooling run at a rate of 20°C min^{-1}, as shown in *Figure 7*. The lower temperature (T_c) transition corresponds to the crystallization of PHB in the blends, and the higher temperature (T_{im}) one to the phase transformation of HECA from an isotropic phase to a mesophase. Compared with that of pure PHB, the T_cs of PHB in the blends shift to lower temperatures. The supercooling temperature, $\Delta T = T_m - T_c$, which represents kinetic crystallizability, is higher than that of pure PHB, indicating lower kinetic crystallizability of PHB in the blends. This result confirms the influence of the HECA component on PHB crystallization. On the other hand, there is almost no effect of PHB melt on the phase transformation of HECA from an isotropic phase to a mesophase; the T_{im}s of HECA in the blends are constant at 144°C.

Because PHB crystallized completely during the d.s.c. cooling run at the lower rate (20°C min^{-1}), no glass transition or cold crystallization of pure PHB was present during the following d.s.c. heating run (run V). For H8, H6 and H4 blends after melt cooling, cold crystallization peaks were found between the T_g and T_m of PHB during the d.s.c. heating runs (runs III and V).

Table 2 Temperatures (°C) and enthalpy (J g^{-1}) of non-isothermal crystallization and cold crystallization of PHB, and phase transformation of HECA from an isotropic phase to a mesophase

Sample code	Run IV[a]				Run III[b]		Run V[c]	
	T_c	ΔH_c	T_{im}	ΔH_{im}	T_{cc}	ΔH_{cc}	T_{cc}	ΔH_{cc}
H10	84.0	64.6	—	—	53.8	33.5	—	—
H8	61.8	12.8	—	—	56.2	34.2	55.2	17.9
H6	67.4	28.8	144.6	0.87	57.8	25.0	56.7	4.86
H4	66.9	10.8	144.5	1.34	57.8	14.9	57.6	2.26
H2	—	—	144.8	2.32	—	—	—	—
H0	—	—	144.1	2.76	—	—	—	—

[a] Obtained from d.s.c. cooling run at a rate of 20°C min^{-1}
[b] The same as in *Table 1*
[c] The same as in *Table 1*

The d.s.c. curves for the H8 blend in runs III and V are shown in *Figure 1*. The temperatures of cold crystallization (T_{cc}s) show a slight shift with increase in the HECA content. Compared with that of pure PHB, the T_{cc}s of PHB in the blends turn to higher temperatures due to the influence of HECA, during the d.s.c. heating run after the cooling run at a rate of 100°C min^{-1} (run III). The T_{cc}s of PHB in the blends in run V are almost the same as the corresponding samples in run III; however, the enthalpy of cold crystallization (ΔH_{cc}) is much lower than that in run III, as shown in *Table 2*.

From the above results, in spite of no specific interaction between the two blend components, the crystallization of PHB both from the melt and from the glassy state is affected by addition of the HECA component, and the phase morphology of the blend can be controlled by HECA content. Thus, the mechanical properties and biodegradation behaviour can be adjusted.

CONCLUSIONS

With PHB contents above 20%, the melting temperatures of PHB in the blends are independent of the blend composition, and the melting enthalpy of the blend is close to the additive value of the enthalpy of the two components. The positions of the absorptions of hydroxyls of HECA and carbonyls of PHB in the blends are independent of the blend composition. The glass transition temperatures of PHB in the blends remain constant at about 8°C. There is almost no effect of the PHB melt on the phase transformation of HECA from an isotropic phase to a mesophase. However, the crystallization of PHB in the blends is affected by the HECA component both from the melt and from the glassy state. Compared with that of pure PHB, the temperatures of non-isothermal crystallization shift to lower temperatures, and the temperatures of cold crystallization to higher temperatures.

ACKNOWLEDGEMENTS

The authors are grateful to the National Natural Science Foundation of China, Postdoctoral Science Foundation of China and National Key Laboratory of Engineering Plastics, Institute of Chemistry, Academia Sinica, for financial support of this work.

REFERENCES

1. Doi, Y., *Microbial Polyesters*. VCH Publishers, New York, 1990.
2. Anderson, A. J. and Dawes, E. A., *Microbiol. Rev.*, 1990, **54**, 450.
3. Holmes, P. A., *Phys. Technol.*, 1985, **16**, 32.
4. Howells, E. R., *Chem. Ind.*, 1982, (Aug.), 508.
5. Barham, P. J. and Keller, A., *J. Polym. Sci., Polym. Phys. Ed.*, 1986, **24**, 69.
6. Doi, Y., *Macromol. Chem. Phys., Macromol. Symp.*, 1995, **98**, 585.
7. Hocking, P. J. and Marchessault, R. H., in *Chemistry and Technology of Biodegradable Polymers*, ed. G. J. L. Griffin. Chapman & Hall, London, 1994, pp. 48–96.
8. Verhoogt, H., Ramsay, B. A. and Favis, B. D., *Polymer*, 1994, **35**, 5155.
9. Avella, M. and Martuscelli, E., *Polymer*, 1988, **29**, 1731.
10. Avella, M., Martuscelli, E. and Greco, P., *Polymer*, 1991, **32**, 1647.
11. Avella, M., Martuscelli, E. and Raimo, M., *Polymer*, 1993, **34**, 3234.
12. Yoon, J. S., Choi, C. S., Maing, S. J., Choi, H. J., Lee, H.-S. and Choi, S. J., *Eur. Polym. J.*, 1993, **29**, 1359.
13. Choi, H. J., Park, S. H., Yoon, J. S., Lee, H.-S. and Choi, S. J., *Polym. Eng. Sci.*, 1995, **35**, 1636.
14. Azuma, Y., Yoshie, N., Sakurai, M., Inoue, Y. and Chûjô, R., *Polymer*, 1992, **33**, 4763.
15. Yoshie, N., Azuma, Y., Sakurai, M. and Inoue, Y., *J. Appl. Polym. Sci.*, 1995, **56**, 17.
16. Blümm, E. and Owen, A. J., *Polymer*, 1995, **36**, 4077.
17. Zhang, L. L., Xiong, C. D. and Deng, X. M., *Polymer*, 1996, **37**, 235.
18. Gassner, F. and Owen, A. J., *Polymer*, 1994, **35**, 2233.
19. Lisuardi, A., Schoenberg, A., Gada, M., Gross, R. A. and McCarthy, S. P., *Polym. Mater. Sci. Eng.*, 1992, **67**, 298.
20. Zhang, L. L. and Deng, X. M., *Polym. Mater. Sci. Eng.*, 1994, **10**, 64 (in Chinese).
21. Abe, H., Doi, Y. and Kumagai, Y., *Macromolecules*, 1994, **27**, 6012.
22. Pearce, R., Jesudason, J., Orts, W., Marchessault, R. H. and Bloembergen, S., *Polymer*, 1992, **33**, 4647.
23. Pearce, R., Brown, G. R. and Marchessault, R. H., *Polymer*, 1994, **35**, 3984.
24. Pearce, R. and Marchessault, R. H., *Polymer*, 1994, **35**, 3990.
25. Organ, S. J. and Barham, P. J., *Polymer*, 1993, **34**, 459.
26. Organ, S. J., *Polymer*, 1994, **35**, 86.
27. Satoh, H., Yoshie, N. and Inoue, Y., *Polymer*, 1994, **35**, 286.
28. Abe, H., Doi, Y., Satkowski, M. M. and Noda, I., *Macromolecules*, 1994, **27**, 50.
29. Scandola, M., Ceccorulli, G. and Pizzoli, M., *Macromolecules*, 1992, **25**, 6441.
30. Ceccorulli, G., Pizzoli, M. and Scandola, M., *Macromolecules*, 1993, **26**, 6722.
31. Tomasi, G. and Scandola, M., *J.M.S.—Pure Appl. Chem.*, 1995, **A32**, 671.
32. Huang, Y., *J. Appl. Polym. Sci.*, 1994, **51**, 1979.
33. Zhao, S. J., Fan, C. Y., Hu, X., Chen, J. R. and Feng, H. F., *Appl. Biochem. Biotechnol.*, 1993, **39/40**, 191.
34. Akita, S., Einaga, Y., Miyaki, Y. and Fujita, H., *Macromolecules*, 1976, **9**, 774.